

Full Length Research Paper

Chemically reacting MHD boundary layer flow of heat and mass transfer over a moving vertical plate with suction

S. Y. Ibrahim^{1*} and O. D. Makinde²

¹Department of Mechanical Engineering, Tamale Polytechnic, Ghana.

²Faculty of Engineering, Cape Peninsula University of Technology, P. O. Box 1906, Bellville 7535, South Africa.

Accepted 13 September, 2010

A mathematical model is presented for a two-dimensional, steady, incompressible electrically conducting, laminar free convection boundary layer flow of a continuously moving vertical porous plate in a chemically reactive medium in the presence of a transverse magnetic field. The basic equations governing the flow are in the form of partial differential equations and have been reduced to a set of non-linear ordinary differential equations by applying suitable similarity transformations. The problem is tackled numerically using shooting techniques with the fourth order Runge-Kutta integration scheme. Pertinent results with respect to embedded parameters are displayed graphically for the velocity, temperature and concentration profiles and were discussed quantitatively.

Key words: Free convection, moving porous plate, magneto-hydrodynamics (MHD), Chemical reaction, heat and mass transfer.

INTRODUCTION

The applications of hydromagnetic incompressible viscous flow in science and engineering involving heat and mass transfer under the influence of chemical reaction is of great importance to many areas of science and engineering. This frequently occurs in petro-chemical industry, power and cooling systems, chemical vapour deposition on surfaces, cooling of nuclear reactors, heat exchanger design, forest fire dynamics and geophysics as well as in magnetohydrodynamic power generation systems. Many analytical and numerical studies have been conducted to explain the various aspects of boundary layer flow with heat and mass transfer over flat surfaces using both Darcian and non-Darcian models for the porous medium drag effects.

Sakiadis (1961) studied the boundary layer flow over a stretching surface moving with a constant velocity, while Tsou et al. (1967) experimentally confirmed the numerical results of Sakiadis by analyzing the effects of heat

transfer on a continuously moving surface with constant velocity. Sakiadis works was extended by Erickson et al. (1966) to include blowing or suction at the stretching sheet on a continuously moving surface with constant speed and investigated its effects on the heat and mass transfer in the boundary layer region. The free-convection flow with thermal radiation and mass transfer over a moving vertical porous plate was investigated by Makinde (2005), whilst laminar free convection flow from a continuously-moving vertical surface in a thermally-stratified non-Darcian high-porosity medium was presented by Beg et al. (2008).

Makinde (2001, 2003, 2008, 2009) have presented some works on the subject of magnetohydrodynamics (MHD) convection in porous medium. The problem of magnetohydrodynamic natural convection about a vertical impermeable flat plate can be found in Sparrow and Cess (1961), (1964) and Pop and Postelnicu (1999). Bakier et al. (1997) presented non-similar solutions for free convection from a vertical permeable plate in porous media whilst Yih (1999) studied the free convection effect on MHD coupled heat and mass transfer of a moving

*Corresponding author. E-mail: yakubuseini@yahoo.com.

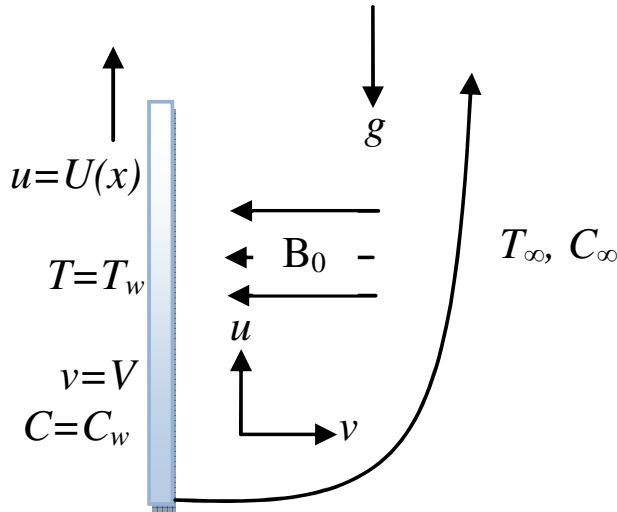


Figure 1. Physical configuration and coordinate system.

permeable vertical surface.

The present communication considers the effects of chemical reaction on a free convection of a continuously moving porous vertical surface as presented in Makinde (2005) and Beg et al. (2008). It investigates numerically the effects of heat and mass transfer in a hydromagnetic boundary layer flow of a moving vertical porous plate with uniform heat generation and chemical reaction. In the problem formulation, the continuity, momentum, energy and concentration equations are reduced to some parameter problem by introducing suitable transformation variables. The equations that govern the flow are coupled and solved numerically using the Newton–Raphson shooting method alongside the fourth-order Runge–Kutta integration scheme. The effects of various flow controlling parameters such as velocity, temperature and concentration are presented graphically and discussed quantitatively. The local skin-friction coefficient and the heat and mass transfer results are illustrated for representative values of the major parameters.

FORMULATION OF THE PROBLEM

Consider a two-dimensional free convection effects on the steady incompressible laminar MHD heat and mass transfer characteristics of a linearly started porous vertical plate, the velocity of the fluid far away from the plate surface is assumed zero for a quiescent state fluid. The variations of surface temperature and concentration are linear. The flow configuration and coordinate system are shown in Figure 1.

All the fluid properties are assumed to be constant except for the density variations in the buoyancy force term of the linear momentum equation. The magnetic Reynolds number is assumed to be small, so that the induced magnetic field is neglected. No electrical field is assumed to exist and both viscous and magnetic dissipations are neglected. The Hall effects, the viscous dissipation and the joule heating terms are also neglected. Under these assumptions, along with Boussinesq approximations, the boundary

layer equations describing this flow as:

$$\frac{\partial u}{\partial x} + \frac{\partial v}{\partial y} = 0 \quad (1)$$

$$u \frac{\partial u}{\partial x} + v \frac{\partial u}{\partial y} = \nu \frac{\partial^2 u}{\partial y^2} + g\beta_T(T - T_\infty) + g\beta_c(C - C_\infty) - \frac{\sigma B_0^2}{\rho} u \quad (2)$$

$$u \frac{\partial T}{\partial x} + v \frac{\partial T}{\partial y} = \alpha \frac{\partial^2 T}{\partial y^2} \quad (3)$$

$$u \frac{\partial C}{\partial x} + v \frac{\partial C}{\partial y} = D \frac{\partial^2 C}{\partial y^2} \quad (4)$$

where u and v are the velocity components in x - and y - directions, respectively. T is the temperature, β_T is the volumetric coefficient of thermal expansion, α is the thermal diffusivity, g is the acceleration due to gravity, ν is the kinematic viscosity, D is the coefficient of diffusion in the mixture, C is the species concentration, σ is the electrical conductivity, B_0 is the externally imposed magnetic field in the y - direction. The relevant boundary conditions can be written as:

$$\begin{aligned} v = V, u = Bx, T = T_w = T_\infty + ax, C = C_w = C_\infty + bx, \\ \text{at } y = 0, \\ u \rightarrow 0, T \rightarrow T_\infty, C \rightarrow C_\infty \text{ as } y \rightarrow \infty, \end{aligned} \quad (5)$$

where B is a constant, a and b denotes the stratification rate of the gradient of ambient temperature and concentration profiles. We introduce the following non-dimensional variables:

$$\begin{aligned} \eta = \sqrt{\frac{B}{\nu}} y, \quad F(\eta) = \frac{\psi}{x\sqrt{B\nu}}, \\ \theta(\eta) = \frac{T - T_\infty}{T_w - T_\infty}, \quad \phi(\eta) = \frac{C - C_\infty}{C_w - C_\infty}, \end{aligned} \quad (6)$$

where $F(\eta)$ is a dimensionless stream function, $\theta(\eta)$ is a dimensionless temperature of the fluid in the boundary layer region, $\phi(\eta)$ is a dimensionless species concentration of the fluid in the boundary layer region and η is the similarity variable. The velocity components u and v are respectively obtained as follows:

$$u = \frac{\partial \psi}{\partial y} = xBF', \quad v = -\frac{\partial \psi}{\partial x} = -\sqrt{B\nu}F, \quad (7)$$

where $F_w = V / \sqrt{B\nu}$ is the dimensionless suction velocity. With this new set of independent and dependent variables defined by Equation (6), the partial differential Equations (2) to (4) are transformed into local similarity equations as follows:

$$F''' + FF'' - (F' + M)F' + G_T\theta + G_C\phi = 0 \quad (8)$$

$$\theta'' + \text{Pr}(F\theta' - F'\theta) = 0 \tag{9}$$

$$\phi'' + \text{Sc}(F\phi' - F'\phi) = 0 \tag{10}$$

where primes denote differentiation with respect to η . The appropriate flat plate and free convection boundary conditions are also transformed into the form:

$$F' = 1, F = -F_w, \theta = 1, \phi = 1 \text{ at } \eta = 0, \tag{11}$$

$$F' = 0, \theta = 0, \phi = 0 \text{ as } \eta \rightarrow \infty,$$

where

$$M = \frac{\sigma B_0^2}{\rho B}$$
 is the magnetic parameter,

$$\text{Pr} = \frac{\nu}{\alpha}$$
 is the Prandtl number,

$$\text{Sc} = \frac{\nu}{D}$$
 is the Schmidt number,

$$G_T = \frac{g\beta_T(T_w - T_\infty)}{xB^2}$$
 is the local temperature Grashof number,

$$G_C = \frac{g\beta_C(C_w - C_\infty)}{xB^2}$$
 is the local concentration Grashof number.

NUMERICAL PROCEDURE

The set of Equations (8) to (10) under the boundary conditions (11) have been solved numerically using the Runge–Kutta integration scheme with a modified version of the Newton–Raphson shooting method. We let $F = x_1, F' = x_2, F'' = x_3, \theta = x_4, \theta' = x_5, \phi = x_6, \phi' = x_7$. Equations (8) to (10) are transformed into systems of first order differential equations as follows:

$$\begin{aligned} x_1' &= x_2, \\ x_2' &= x_3, \\ x_3' &= -x_1x_3 + x_2^2 + Mx_2 - G_Tx_4 - G_Cx_6, \\ x_4' &= x_5, \\ x_5' &= -\text{Pr}x_1x_5 + \text{Pr}x_2x_4, \\ x_6' &= x_7, \\ x_7' &= -\text{Sc}x_1x_7 + \text{Sc}x_2x_6, \end{aligned} \tag{12}$$

subject to the following initial conditions:

$$\begin{aligned} x_1(0) &= -F_w, \quad x_2(0) = 1, x_3(0) = s_1, \\ x_4(0) &= 1, x_5(0) = s_2, x_6(0) = 1, x_7(0) = s_3. \end{aligned} \tag{13}$$

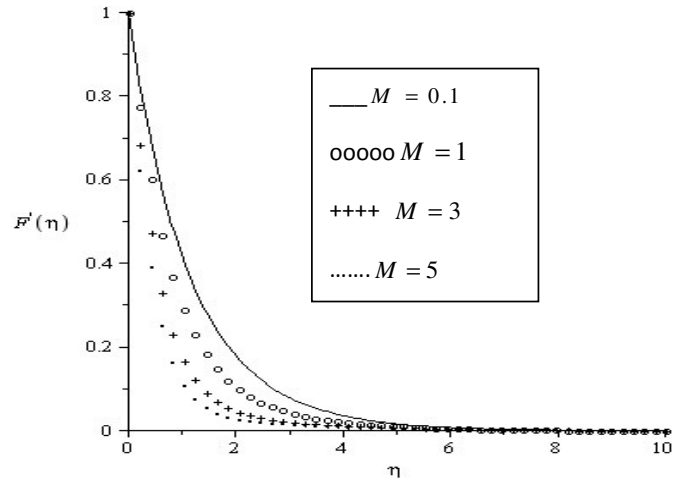


Figure 2. Velocity profile for $\text{Pr} = 0.72, \text{Sc} = 0.62, F_w = G_T = G_C = 0.1$.

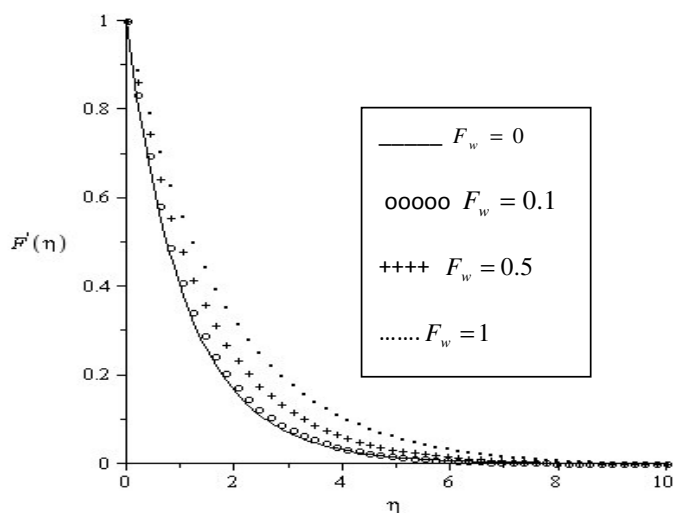
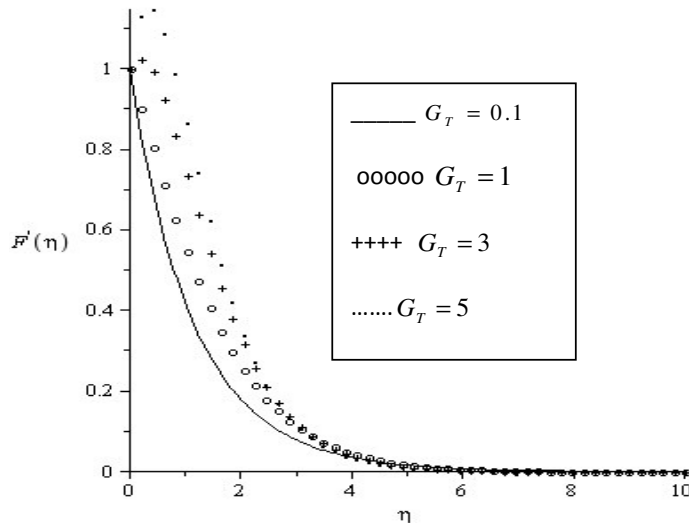
In a shooting method, the unspecified initial conditions; s_1, s_2 and s_3 in Equation (13) are assumed. Equation (12) is then integrated numerically as an initial valued problem to a given terminal point. The accuracy of the assumed missing initial condition is then checked by comparing the calculated value of the dependent variable at the terminal point with its given value. If a difference exists, improved values of the missing initial conditions must be obtained and the process is repeated. The computations were done by a written program, which uses a symbolic and computational computer language MAPLE. A step size of $\Delta\eta = 0.001$ was selected to be satisfactory for a convergence criterion of 10^{-7} in nearly all cases. The maximum value of η_{∞} , to each group of parameters $\text{Sc}, M, G_T, G_C,$ and Pr are determined when the values of unknown boundary conditions at $\eta = 0$ does not change to successful loop with error less than 10^{-7} . From the process of numerical computation, the local skin friction coefficient, the local Nusselt number and the local Sherwood number, which are respectively proportional to $F''(0), -\theta'(0),$ and $-\phi'(0)$ are worked out and their numerical values presented in a tabular form.

RESULTS

Numerical results are reported in the Table 1 and Figures 2 to 17. The Prandtl number was taken to be $\text{Pr} = 0.72$, which corresponds to air, the values of Schmidt number (Sc) were chosen to be $\text{Sc} = 0.24, 0.62, 0.78, 2.62$, representing diffusing chemical species of most common interest in air like $\text{H}_2, \text{H}_2\text{O}, \text{NH}_3,$ and Propyl Benzene, respectively. Attention is focused on positive values of the buoyancy parameters, that is, Grashof number $G_T > 0$ (which corresponds to the cooling problem) and solutal Grashof number $G_C > 0$ (which indicates that the chemical species concentration in the free stream region is less than the concentration at the boundary surface). From Table 1, it is important to note that the skin friction together with the heat and mass transfer rate at the moving plate surface decreases with increasing

Table 1. Computation showing $f''(0)$, $\phi'(0)$ and $\theta'(0)$ for various values of embedded parameter $Pr = 0.72$.

G_T	G_c	M	F_w	Sc	$F''(0)$	$-\theta'(0)$	$-\phi'(0)$
0.1	0.1	0.1	0.1	0.62	0.888971	0.7965511	0.7253292
0.5	0.1	0.1	0.1	0.62	0.695974	0.8379008	0.7658018
1.0	0.1	0.1	0.1	0.62	0.475058	0.8752835	0.8020042
0.1	0.5	0.1	0.1	0.62	0.686927	0.8421370	0.7701717
0.1	1.0	0.1	0.1	0.62	0.457723	0.8818619	0.8087332
0.1	0.1	1.0	0.1	0.62	1.264488	0.7089150	0.6400051
0.1	0.1	3.0	0.1	0.62	1.868158	0.5825119	0.5204793
0.1	0.1	0.1	1.0	0.62	0.570663	0.5601256	0.5271504
0.1	0.1	0.1	3.0	0.62	0.275153	0.2955702	0.2902427
0.1	0.1	0.1	0.1	0.78	0.893454	0.7936791	0.8339779
0.1	0.1	0.1	0.1	2.62	0.912307	0.7847840	1.6504511

**Figure 3.** Velocity profile for $Pr = 0.72$, $Sc = 0.62$, $M = G_T = G_c = 0.1$.**Figure 4.** Velocity profiles for $Pr = 0.72$, $Sc = 0.62$, $M = F_w = G_c = 0.1$.

magnitude of fluid suction (F_w) at the moving surface. The rate of heat and mass transfer at the plate surface increases with increasing intensity of buoyancy forces (G_T , G_c) and decreases with increasing intensity of magnetic field (M). Moreover, the skin friction decreases with buoyancy forces and increases with increasing magnetic field intensity and Schmidt number (Sc). Furthermore, the surface mass transfer rate increases, while the surface heat transfer rate decreases with an increase in the Schmidt number (Sc).

DISCUSSION

Effects of parameter variation on velocity profiles

Generally, the fluid velocity is higher near the moving

surface and decreases to its zero value far away from the plate surface satisfying the far field boundary condition for all parameter values. In Figure 2, the effect of increasing the magnetic field strength on the momentum boundary-layer thickness is illustrated. It is now a well established fact that the magnetic field presents a damping effect on the velocity field by creating a drag force that opposes the fluid motion, causing the velocity to decrease. Figure 3 shows an increase in the fluid velocity within the boundary layer due to suction. Similar trend is observed with an increase in the buoyancy forces parameters (G_T , G_c). However, as shown in Figures 4 and 5, an upward acceleration of the fluid in the vicinity of the vertical wall is observed with increasing intensity of buoyancy forces. Further, downstream of the fluid motion decelerates to the free stream

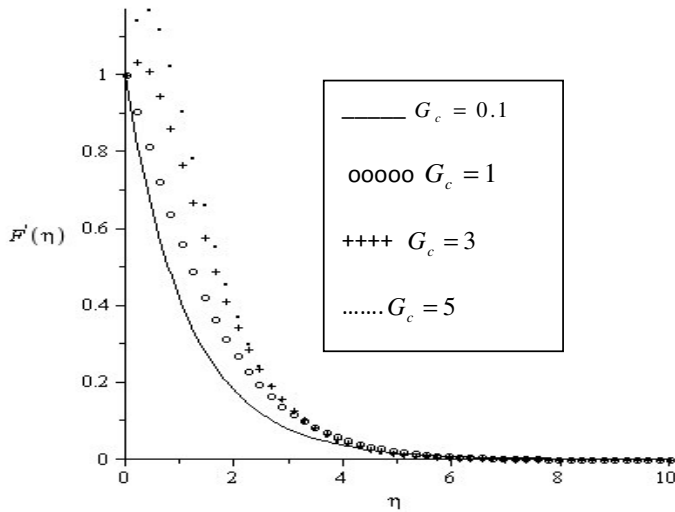


Figure 5. Velocity profiles for $Pr = 0.72$, $Sc=0.62$, $M = F_w = G_T = 0.1$.

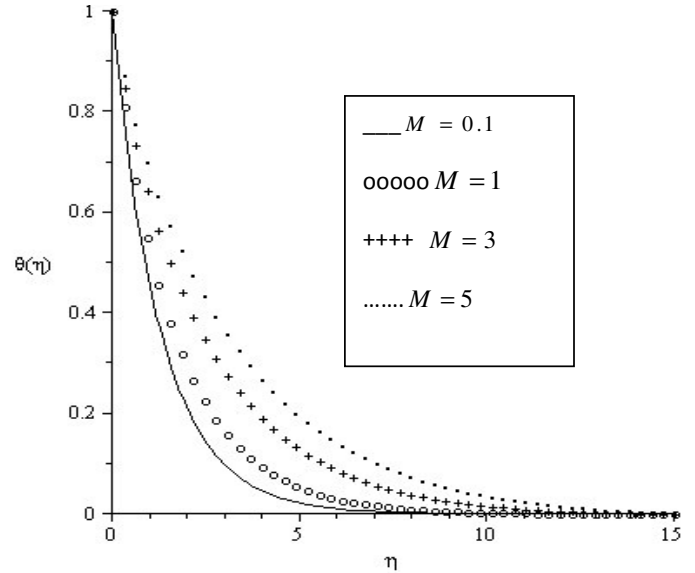


Figure 7. Temperature profiles for $Pr = 0.72$, $Sc = 0.62$, $F_w = G_T = G_c = 0.1$.

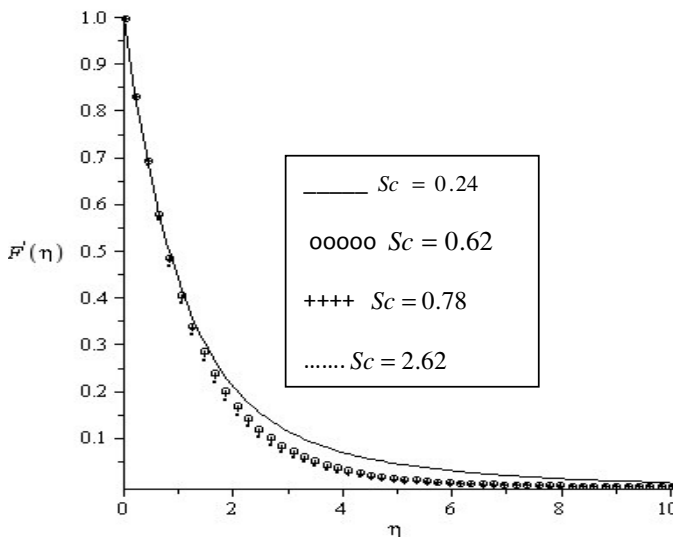


Figure 6. Velocity profiles for $Pr = 0.72$, $M = F_w = G_c = G_T = 0.1$.

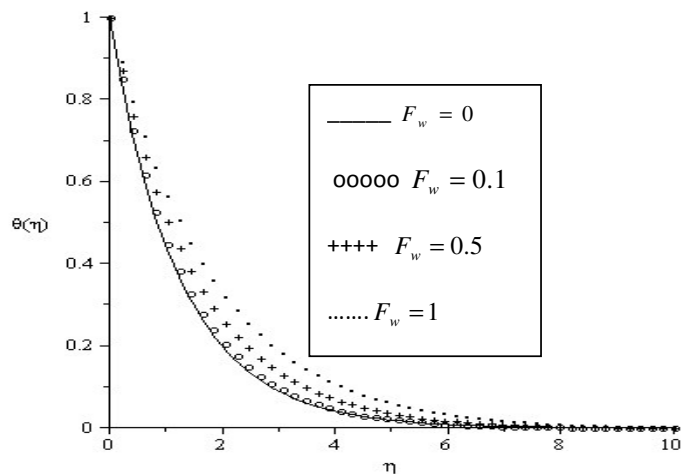


Figure 8. Temperature profile for $Pr = 0.72$, $Sc=0.62$, $M=G_T = G_c = 0.1$.

velocity. Figure 6 shows a slight decrease in the fluid velocity with an increase in Schmidt number.

Effects of parameter variation on temperature profiles

Figures 7 to 12 show that the fluid temperature attains its maximum value at the moving plate surface and decrease exponentially to the free stream zero value away from the plate satisfying the boundary conditions. It is noteworthy that the thermal boundary layer thickness increases with an increase in the intensity of magnetic field (M) and fluid suction. The trend is opposite with an

increase in both thermal and solutal Grashof numbers (Gr_x, Gc_x), that is, a decrease in the fluid temperature is observed with an increase in the intensity of buoyancy force. Moreover, the fluid temperature increases slightly with an increase in the Schmidt number (Sc) leading to a slight increase in thermal boundary layer thickness.

Effects of parameter variation on concentration profiles

Figures 13 to 17 depict chemical species concentration profiles against spanwise coordinate η for varying values physical parameters in the boundary layer. The species

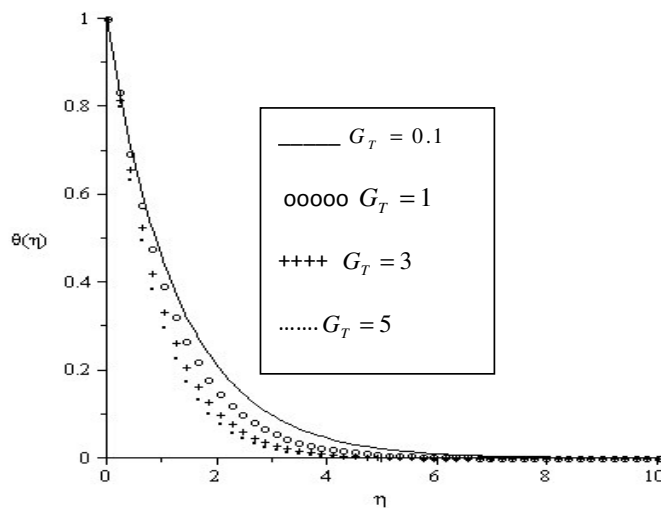


Figure 9. Temperature profiles for $Pr = 0.72$, $Sc = 0.62$, $M = F_w = G_c = 0.1$.

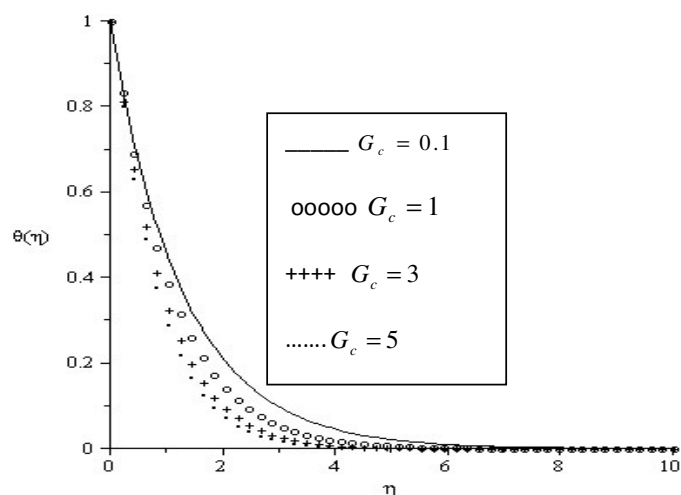


Figure 10. Temperature profiles for $Pr = 0.72$, $Sc = 0.62$, $M = F_w = G_T = 0.1$.

concentration is highest at the moving plate surface and decreases to zero far away from the plate satisfying the boundary condition. From these figures, it is noteworthy that the concentration boundary layer thickness increases with an increase in the magnetic field intensity (M). The same trend is observed with an increase in the magnitude of fluid suction at the moving surface. An increase in the values of both thermal and solutal Grashof numbers due to buoyancy forces causes a decrease in the chemical species concentration within the boundary layer leading to a decaying concentration boundary layer thickness. It is interesting to note that the chemical species concentration also decreases within the boundary layer with an increase in Schmidt number due

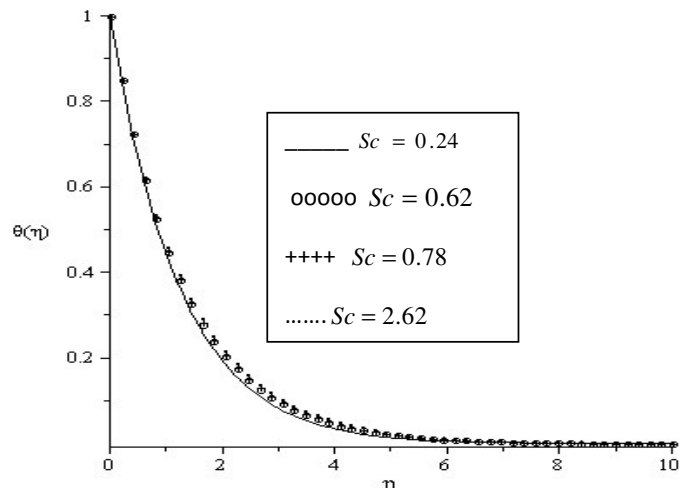


Figure 11. Temperature profile for $Pr = 0.72$, $Gr_x = G_c_x = Ha_x = Bi_x = 0.1$.

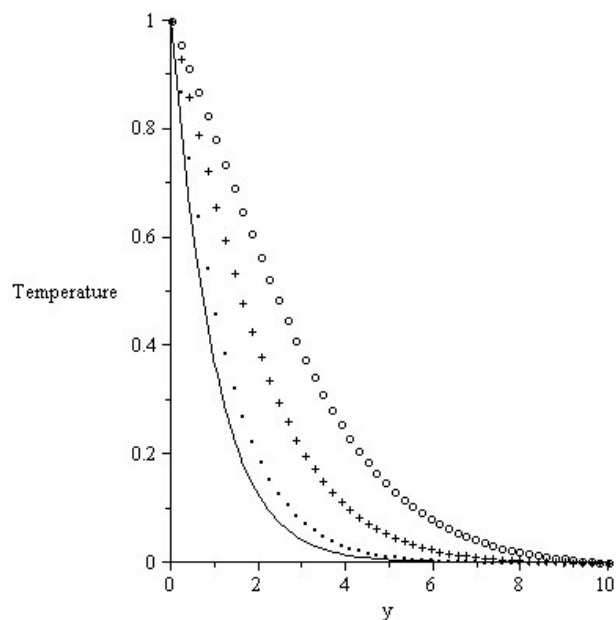


Figure 12. Temperature profile for varying suction parameter when $Pr = 0.72$, $Sc = 0.62$, $Gr_x = G_c_x = 1$, $M = 0.1$.

to the combined effects of buoyancy forces and species molecular diffusivity.

Conclusions

This paper studied the combined effects of wall suction and magnetic field on boundary layer flow with heat and mass transfer over an accelerating vertical plate. The governing equations are approximated to a system of non-linear ordinary differential equations by similarity

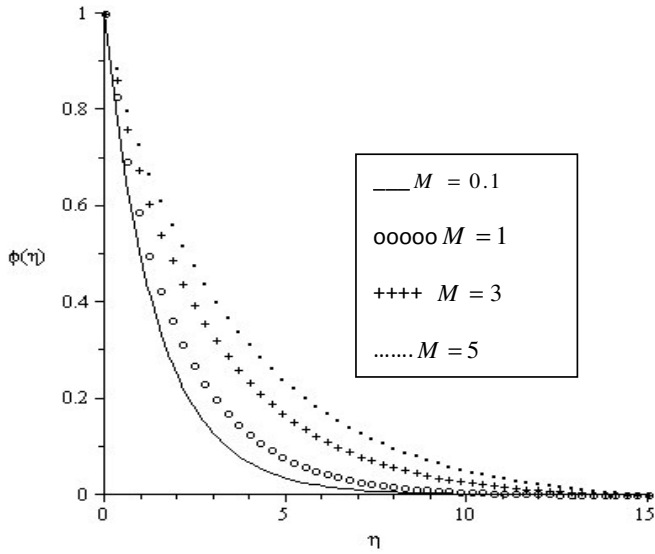


Figure 13. Concentration profiles for $Pr = 0.72$, $Sc = 0.62$, $F_w = G_T = G_c = 0.1$.

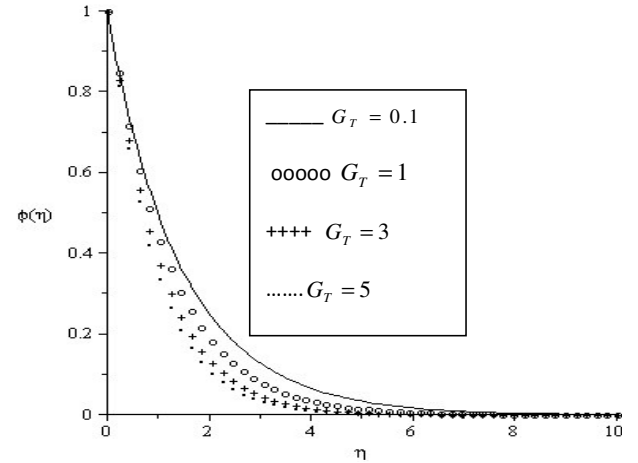


Figure 15. Concentration profiles for $Pr = 0.72$, $Sc = 0.62$, $M = F_w = G_c = 0.1$.

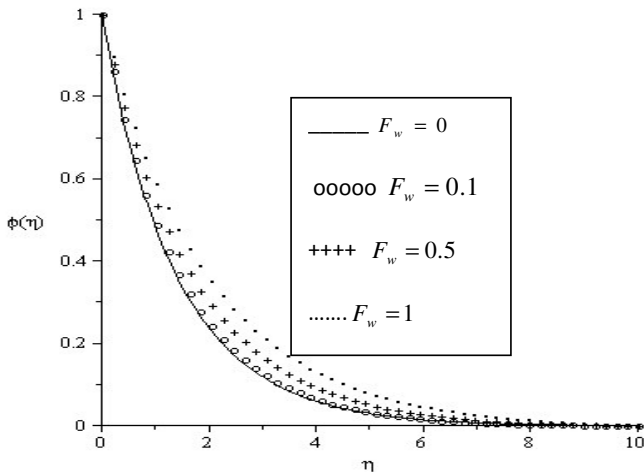


Figure 14. Concentration profiles for $Pr = 0.72$, $Sc = 0.62$, $M = G_T = G_c = 0.1$.

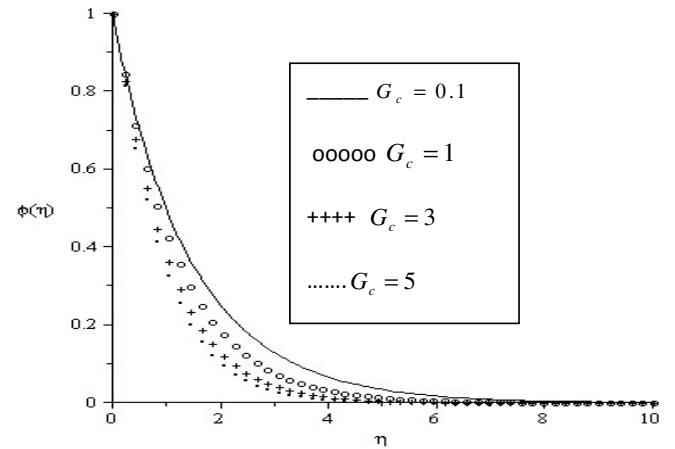


Figure 16. Concentration profiles for $Pr = 0.72$, $Sc = 0.62$, $M = F_w = G_T = 0.1$.

transformation. Numerical calculations are carried out for various values of the dimensionless parameters of the problem. Our results revealed that the momentum boundary layer thickness decreases, while both thermal and concentration boundary layer thicknesses increase with an increase in the magnetic field intensity. Furthermore, an increase in wall suction enhances the boundary layer thickness and reduces the skin friction together with the heat and mass transfer rate at the moving plate surface.

REFERENCES

Bakier AY, Mansour MA, Gorla RSR, Ebiana AB (1997). Nonsimilar solutions for free convection from a vertical plate in porous media.

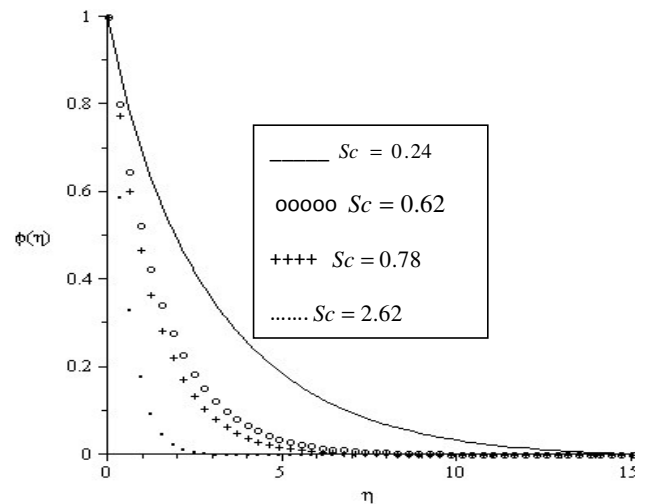


Figure 17. Concentration profiles for $Pr = 0.72$, $Gr_x = G_c = Bi_x = Ha_x = 0.1$.

- Heat Mass Transfer, 33: 145-148.
- Beg OA, Joaquín Zueco, Takhar HS (2008). Laminar free convection from a continuously-moving vertical surface in thermally-stratified non-Darcian high-porosity medium: Network Numerical Study. International Commun. Heat Mass Transfer, 35: 810-816.
- Erickson LE, Fan LT, Fox VG (1966). Heat and Mass transfer in the laminar boundary layer flow of a moving flat surface with constant surface velocity and temperature focusing on the effects of suction/injection, Ind. Eng. Chem., 5: 19-25.
- Makinde OD (2001). MHD steady flow and heat transfer on the sliding plate. A. M. S. E., Modelling, Measure. Control B, 70(1): 61-70.
- Makinde OD (2003). Magneto-Hyromagnetic Stability of plane-Poiseuille flow using Multi-Deck asymptotic technique. Math. Comput. Modelling, 37(3-4): 251-259.
- Makinde OD (2005). Free-convection flow with thermal radiation and mass transfer past a moving vertical porous plate. Int. Commun. Heat Mass Transfer, 32: 1411-1419.
- Makinde OD (2008). Effect of arbitrary magnetic Reynolds number on MHD flows in convergent-divergent channels. Int. J. Num. Meth. Heat Fluid Flow, 18(6): 697-707.
- Makinde OD (2009). On MHD boundary-layer flow and mass transfer past a vertical plate in a porous medium with constant heat flux. Int. J. Num. Meth. Heat Fluid Flow, 19(3/4): 546-554.
- Pop I, Postelnicu A (1999). Similarity solutions of free convection boundary layers over vertical and horizontal surface porous media with internal heat generation. Int. Commun. Heat Mass Transfer, 26: 1183-1191.
- Sakiadis BC (1961). Boundary layer behavior on continuous solid flat surfaces. AIChE J., 7: 26-28.
- Sparrow EM, Cess RD (1961). The effect of a magnetic field on free convection heat transfer. Int. J. Heat Mass Transfer, 4: 267-274.
- Tsou FK, Sparrow EM, Goldstein RJ (1967). Flow and heat transfer in the boundary layer on a continuous moving surface. Int. J. Heat Mass Transfer, 10: 219-235.
- Yih KA (1999). Free convection effect on MHD coupled heat and mass transfer of a moving permeable vertical surface. Int. Commun. Heat Mass Transfer, 26(1): 95-104.